JACS
JOURNAL OF THE AMERICAN CHEMICAL SOCIETY
Article
pubs.acs.org/JACS

Directed Assembly of Nucleic Acid-Based Polymeric Nanoparticles from Molecular Tetravalent Cores

Bong Jin Hong,[†] Ibrahim Eryazici,[†,#] Reiner Bleher,[‡,§] Ryan V. Thaner,[†] Chad A. Mirkin,[†] and SonBinh T. Nguyen*[,†]

[†]Department of Chemistry, Northwestern University, 2145 Sheridan Road, Evanston, Illinois 60208-3113, United States

[‡]Department of Materials Science and Engineering, Northwestern University, 2220 Campus Drive, Evanston, Illinois 60208-3108, United States

[§]NUANCE Center, Northwestern University, 2220 Campus Drive, Evanston, Illinois 60208-3108, United States

Supporting Information

ABSTRACT: Complementary tetrahedral small molecule-DNA hybrid (SMDH) building blocks have been combined to form nucleic acid-based polymeric nanoparticles without the need for an underlying template or scaffold. The sizes of these particles can be tailored in a facile fashion by adjusting assembly conditions such as SMDH concentration, assembly time, and NaCl concentration. Notably, these novel particles can be stabilized and transformed into functionalized spherical nucleic acid (SNA) structures through the incorporation of capping DNA strands conjugated with functional groups. These results demonstrate a systematic, efficient strategy for the construction and surface functionalization of well-defined, size-tunable nucleic acid particles from readily accessible molecular building blocks. Furthermore, because these nucleic acid-based polymeric nanoparticles exhibited enhanced cellular internalization and resistance to DNase I compared to free synthetic nucleic acids, they should have a plethora of applications in diagnostics and therapeutics.

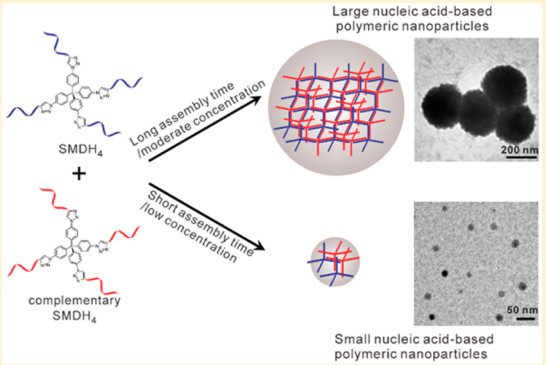

INTRODUCTION

Over the last few decades, DNA has emerged as a key building block for molecular assemblies and nanostructures[1−4] due to the versatile programmability encoded into the base-pairing interactions (A−T and G−C) between complementary strands. Such high specificity and predictability at the molecular level can be readily translated into an exquisite control of assembly interactions at the nanoscale,[5] enabling the formation of a variety of topologically distinct DNA-based constructs such as rings,[6] boxes,[7] tubes,[8] and macroscopic crystals.[9] Recently, well-defined small molecule-DNA hybrids (SMDHs), comprising multiple DNA strands covalently attached to small-molecule cores, have quickly gained popularity as DNA-containing building blocks for nanomaterials with valency that can be tuned through the number and orientation of the strands.[10,11] SMDHs greatly increase the scope and versatility of the design and construction of DNA-based nanostructures because branched building blocks can be made efficiently from relatively short oligonucleotides and a broad range of organic cores. Early work in SMDH-based assembly has often focused on the careful selection of an organic core with three or fewer DNA strands, along with a predesigned sequence and strand orientation of the DNA, to afford thermodynamically stable discrete 2D or 3D supramolecular structures.[12−14] However, when SMDHs with more than three strands are hybridized with their complementary SMDHs, a broad range of ill-defined products can result,[15,16] decreasing the yield of the desired discrete product. Indeed, only macroscopic aggregates were observed in the assembly of self-complementary tetrahedral SMDH building blocks ($SMDH_4$) possessing as few as two base pairs per DNA arm.[15,16]

Herein, we report that the assembly of two complementary $SMDH_4$ building blocks, with four DNA strands around relatively rigid tetrahedral cores, can be readily controlled to yield well-defined, narrowly dispersed spherical nanoparticles (Figure 1). These small particles are almost entirely nucleic acids in composition and their sizes can be tuned easily by controlling nucleic acid concentration, assembly time, and NaCl concentration. Notably, they can be stabilized, and transformed into structures similar to functionalized spherical nucleic acids (SNA), through the incorporation of capping DNA strands conjugated with functional groups. These nanoparticles exhibit efficient cellular uptake compared to the free DNA arms of the $SMDH_4$ building blocks, and show enhanced resistance to a DNase I enzyme when capped with a PEG-functionalized strand. Such characteristics make them highly attractive for applications in both diagnostics and therapeutics.

Received: April 3, 2015
Published: May 17, 2015

DOI: 10.1021/jacs.5b03485
J. Am. Chem. Soc. 2015, 137, 8184−8191

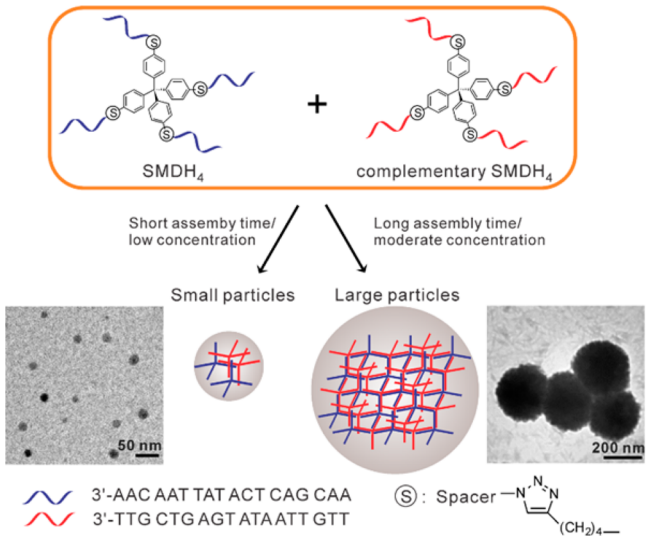

Figure 1. Assembly of nucleic acid-based polymeric nanoparticles from $SMDH_4$ and its complementary partner. Size-tunable particles can be obtained by slow (~0.2 °C/min; right) or fast (~10 °C/min; left) cooling of a "hot" assembly solution (total [DNA] = 15 μM, T = 90 °C), respectively. The "diamond lattice" drawings that were embedded in the spherical cartoons of the nanoparticles are only ideal representations of the network and should not be taken literally.

RESULTS AND DISCUSSION

We and others have previously shown that the hybridization of SMDHs containing more than three DNA strands with their complementary SMDHs at high DNA concentrations (40−150 μM) can result in ill-defined networks[12,17] and visually observable large aggregates.[15,16] However, this outcome can be modulated either with an additive or by changing the flexibility of the spacer between the core and the DNA arms. For example, Sleiman and co-workers have employed a $Ru(bpy)_3^{2+}$ guest template to preferentially induce the formation of fibers over ill-defined networks in the assembly of complementary rigid $SMDH_3$s.[17] Subsequently, we demonstrated that the yields of small discrete cage-like $SMDH_3$ dimers can be greatly increased over those of higher-order aggregates when unhybridized oligo(deoxythymidine) spacers are included between the relatively rigid organic core and the hybridizing DNA arms to provide more flexibility for the assembly to "anneal" into more thermodynamically stable discrete structures.[12] This *spacer flexibility* is particularly important when the hybridizing DNA arms are long or when the total nucleic acid concentration of the assembly is high (>5 μM).[12,18]

Parallel to the aforementioned developments, recent work in the growth of colloidal nanoparticles[19,20] has shown that tuning the assembly conditions—such as concentrations of the components that are participating in the assembly, temperature, and assembly rate—can significantly affect the morphological outcome of an assembly process. Our own work in the assembly of complementary $SMDH_3$s has also indicated that the total concentration of DNA in solution,[12] the annealing rate,[18] and the salt concentrations[12,18] are very important parameters that dictate the proportions of well-defined dimers vs higher-order structures. These results prompted us to hypothesize that discrete nanostructures may be obtained readily from tetrahedral $SMDH_4$ building blocks at low-to-moderate nucleic acid concentrations (2−15 μM) and through a careful control of the assembly conditions.

Direct Assembly of Nucleic Acid-Based Polymeric Nanoparticles from $SMDH_4$ Building Blocks. To test the aforementioned hypothesis, we selected $SMDH_4$ building blocks with a tetraphenylmethane core and 18-base DNA arms that are linked together through $(CH_2)_4$-triazole spacers. From previous studies, we suspected that this design would afford the right combination of stability and flexibility needed for optimizing the formation of discrete nanostructures. To our advantage, these building blocks can be obtained readily in large-enough quantities for our study through a solid-state click coupling strategy that was previously shown[11] to favor multiarm products (see Experimental Section). In an initial screen, equimolar mixtures of the $SMDH_4$ and its complementary partner were combined in Tris-buffered saline (TBS, 20 mM Tris·HCl and 150 mM NaCl buffer solution, pH 7.4) at DNA concentrations in the 2−100 μM range and annealed following established DNA hybridization protocols (see Experimental Section). In a typical annealing procedure, the assembly mixture is heated to 90 °C in a heating block and kept there for 5−10 min to eliminate all initial DNA interactions; turning off the heating block then allows the mixture to slowly cool to rt over 3 h and for DNA-hybridized colloidal aggregates to form. These aggregates were then examined by dynamic light scattering (DLS), which reports the hydrodynamic diameter (D_H) of the particles *in solution*, and scanning transmission electron microscopy (STEM), which reflects the sizes and shapes for the particles *in a vacuum*.

While the assemblies at high SMDH concentrations (total [DNA] = 100 μM) yielded only macroscopic aggregates (Supporting Information (SI), Figure S3), as reported previously;[15,16] those at lower concentrations (total [DNA] = 2−15 μM) afforded well-defined, narrowly dispersed particles (Figure 2). At 15 μM total nucleic acid concentration, the average D_H of the assembled particles is 360 ± 60 nm, while that at 2 μM concentration is a remarkably small 24 ± 6 nm. Together with these DLS data (Figure 2a), agarose gel electrophoresis analysis (SI, Figure S4) confirms that these

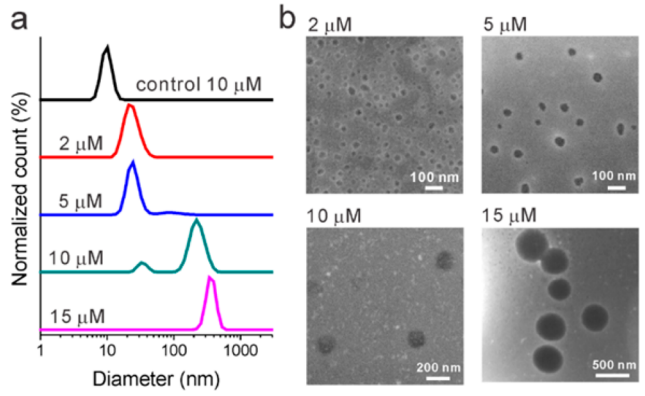

Figure 2. Effect of SMDH concentration on the size of assembled nucleic acid-based polymeric nanoparticles in TBS. The nucleic acid-based polymeric nanoparticles were prepared with a 1:1 ratio of $SMDH_4$ and its complementary partner using an established DNA hybridization method (see Experimental Section). The average sizes of the particles were determined by (a) DLS and (b) STEM. The concentration values listed above the DLS graphs and STEM images are the total DNA concentrations present (4 × [$SMDH_4$], as there are four DNA strands in each $SMDH_4$ molecule) in the assembly solution. The "control" sample was a $SMDH_4$ that hybridized with 4 equiv of complementary ssDNA under the same assembly condition.

DOI: 10.1021/jacs.5b03485
J. Am. Chem. Soc. 2015, 137, 8184−8191

small particles are completely different from the species formed by hybridizing one of our $SMDH_4$ building blocks with the complementary single-stranded (ss)DNA. The STEM images (Figure 2b) of the assembled products support the DLS results and show all particles are spherical in shape. In addition, the particles prepared at high concentration (total [DNA] = 15 μM) cannot be converted to smaller particles when diluted to similarly low concentration (total [DNA] = 2 μM; SI, Figure S5), suggesting that the individual SMDH components in the assembled particles are strongly connected to each other.

When the assemblies were carried out at temperatures well above 57 °C, the characteristic melting temperature (T_m) of the hybridized products between $SMDH_4$ and its complementary partner (SI, Figure S6), the hybridization interactions between the arms are not stable and both SMDHs remain apart in solution. As the temperature of the assembly mixture is decreased toward T_m, duplex formation between the DNA arms on adjacent molecules begins to link them together, forming oligomers and small polymeric nanoparticles. If the total DNA concentration in the initial mixture is high, hybridization occurs in a fast, unoptimized manner throughout the mixture, which will result in large aggregates.[15,16] However, if the total DNA concentration in the initial mixture is low, the $SMDH_4$ concentration around the nucleation sites can be quickly depleted and the probability for forming large aggregates decreases, just as in condensation polymerization. This represents an opportunity for the nanoscale $SMDH_4$ particles to be "trapped" in a kinetically stable state. If this process is further controlled in a way that does not allow neighboring nanoparticles to undergo aggregation, they would remain as discrete entities. Within this kinetically stable regime, the size of the nanoparticles should be easily tuned by varying the initial DNA concentration and the cooling rate.

Expanding upon the aforementioned idea of controllable kinetic trapping, fast cooling (short assembly time) near T_m should decrease the number of collisions between neighboring particles, resulting in a stable population of smaller particles. In contrast, prolonged cooling (long assembly time) near T_m should correspond to more collisions and give rise to larger particles. To evaluate this effect, an equimolar mixture of the two $SMDH_4$ components (total [DNA] = 10 μM) was prepared in TBS. After being heated at 90 °C for 10 min in a thermal cycler, this mixture was cooled down to room temperature at different rates (5.5, 1.0, 0.34, and 0.17 °C/min) and monitored using DLS. As shown in Figure 3a, the particles obtained in the fast-cooled (5.5 °C/min) solution are much smaller (D_H = 23 ± 7 nm) than those obtained from the slow-cooled (0.17 °C/min) solution (D_H = 300 ± 80 nm). As the cooling rate decreased from 5.5 °C/min, bimodal populations of larger and larger nanoparticles were observed. Correspondingly, the STEM images of all mixtures show spherically shaped nanoparticles. Not only do these results confirm that the size of the nucleic acid-based polymeric nanoparticles can indeed be modulated by the assembly time, they also suggest that the small particles that were previously observed only at low concentrations (total [DNA] ≤ 5 μM) could now be successfully synthesized at moderate concentrations (total [DNA] up to 15 μM; see SI, Figure S7) with fast cooling.

In addition to the total DNA concentration and the assembly time, the concentration of Na^+ ions in the assembly solutions also has significant effects on the average size of the assembled particles. As shown in Figure 4a, higher [NaCl] leads to larger

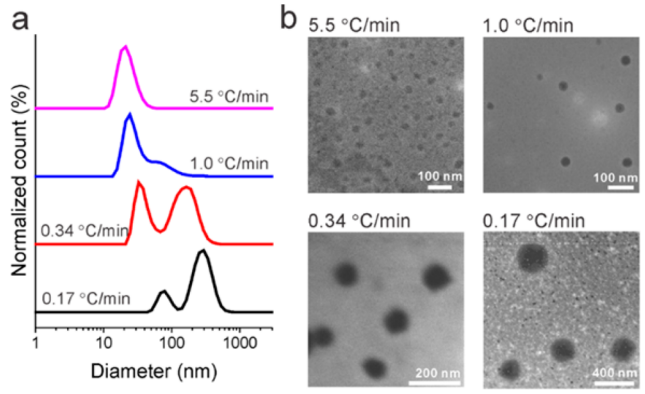

Figure 3. Effect of the assembly time on the size of assembled nucleic acid-based polymeric nanoparticles. Equimolar solutions of $SMDH_4$ and its complementary partner (total [DNA] = 10 μM) were heated at 90 °C for 10 min in a thermal cycler and then cooled down at different rates as indicated above the DLS graphs (a) and STEM images (b) of the samples.

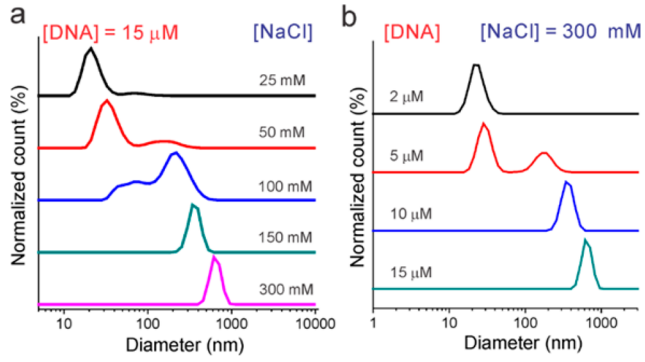

Figure 4. Effect of [NaCl] on the size of assembled nucleic acid-based polymeric nanoparticles. (a) D_H data for particles prepared by combining equimolar quantities of the SMDH components (total [DNA] = 15 μM) in solutions with different concentrations of Na^+ ions ([NaCl] = 25, 50, 100, 150, and 300 mM). Data for the particles prepared with total [DNA] = 10 μM can be found in the SI, Figure S8. (b) D_H data for particles prepared by combining equimolar quantities of the SMDHs at different DNA concentrations (total [DNA] = 2, 5, 10, and 15 μM) and at [NaCl] = 300 mM. The [NaCl] and total [DNA] are indicated above each graph and the D_H of the particles was determined by DLS.

particles: the D_H of the particles is 650 ± 100 nm at 300 mM NaCl, and 25 ± 12 nm at 25 mM NaCl. This is not surprising when one considers that Na^+ ions can increase the rate of duplex formation, as well as the stability of the final duplex, by reducing the repulsive force between the negatively charged DNA strands. Interestingly, the magnitude of the effect of [NaCl] depends significantly on the concentration of the SMDHs. At low SMDH concentration (total [DNA] = 2 μM), the average diameters of the particles at high (300 mM) and low (50 mM) [NaCl] are not significantly different (cf. the top DLS profile in Figure 4b and the top DLS profile in Figure S9 in the SI). In contrast, the particles prepared at >2 μM total [DNA] show significant variations in size and population distributions when the [NaCl] varies (cf. the lower DLS profiles in Figure 4b and the lower DLS profiles in Figures S9 in the SI). These results suggest that while increasing the [NaCl] can increase the size of nucleic acid-based polymeric nanoparticles, through either aggregation or Ostwald ripening,

DOI: 10.1021/jacs.5b03485
J. Am. Chem. Soc. 2015, 137, 8184–8191

there is a minimal SMDH concentration required before this effect becomes significant.

Stability and Facile Surface Functionalization of Nucleic Acid-Based Polymeric Nanoparticles. Because our nucleic acid-based polymeric nanoparticles were derived from two complementary components, their surfaces have an approximately equal population of two types of complementary DNA strands that do not hybridize with each other due to steric constraints. However, as expected for kinetically stabilized species, the as-prepared particles continue to aggregate over the next 4 weeks at room temperature through hybridization events between unhybridized strands on the surfaces of neighboring particles (Figure 5, top path). This propensity to aggregate can

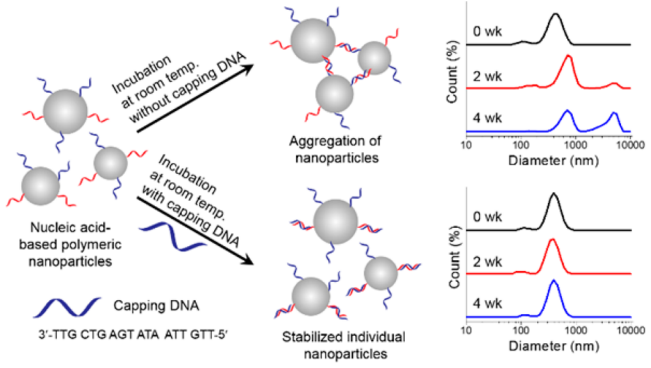

Figure 5. (Left) Schematic illustration of the capping-stabilization experiment. (Right) Comparative D_H data (determined by DLS) for nucleic acid-based polymeric nanoparticles formed from an equimolar mixture of $SMDH_4$ and its complementary partner (total [DNA] = 15 μM) at rt without (top) and with (bottom) capping DNA (added [DNA] = 7.5 μM). The incubation times are indicated above each graph (wk = week).

be minimized by capping one of these two types of unhybridized strands with complementary ssDNA strands, leading to particles that are fully stabilized for over 4 weeks (Figure 5, bottom path). This advance not only is important for stabilization purposes, but also transforms these nucleic acid materials into novel forms of spherical nucleic acids (SNAs),[2] which have become extremely important as building blocks in materials science,[21,22] labels in in vitro and intracellular diagnostics,[23] and delivery agents in therapeutic applications.[24]

The availability of two different types of complementary DNA strands on the surface of our nucleic acid-based polymeric nanoparticles also makes it an excellent platform for orthogonal functionalization. One of these strands can be capped with a functionalized ssDNA and the remaining uncapped DNA strand can subsequently be modified with a second set of functionalized capping strands; the whole platform would then bear two different functional groups. As a proof-of-concept experiment, an Alexa Fluor 647 (AF647)-conjugated capping DNA strand (5 μM) that hybridizes with the remaining unbound strands of $SMDH_4$ on the surface of the particles was added to a solution of as-prepared particles (equimolar amounts of $SMDH_4$ and its complementary partner; total [DNA] = 10 μM) and incubated at room temperature for 8 h (Figure 6a). Examining the resulting solutions by confocal laser scanning microscopy (CLSM) at room temperature clearly shows bright fluorescent dots against a darker background (Figure 6a), suggesting the presence of individual spherical particles that concentrated the AF647 fluorophores. This is in

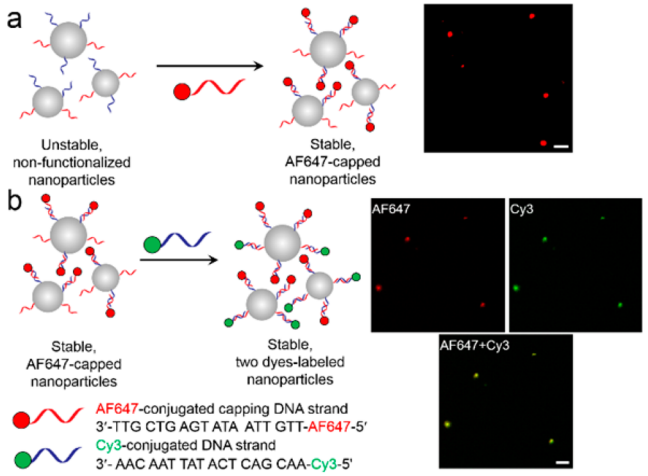

Figure 6. Orthogonal incorporation of two dyes (AF647 and Cy3) into nucleic acid-based polymeric nanoparticles. The particles were first prepared from an equimolar mixture of $SMDH_4$ and its complementary partner (total [DNA] = 10 μM). They were then sequentially mixed with (a) AF647-labeled and (b) Cy3-labeled capping DNA strands (added [DNA] = 5 μM each) at room temperature. CLSM images were obtained at each step as shown on the right side of each panel (scale bars are 2 μm). In panel b, the left and right images at the top are obtained at the fluorescent emission wavelengths for AF647 (shown as red) and Cy3 (shown as green) dyes, respectively; the image at the bottom is the colocalized fluorescence image of these top two, suggesting effective orthogonal functionalization.

clear contrast to the uniform, nondistinct image of a control solution of only AF647 capping strands (SI, Figure S10). As expected, these AF647-capped particles exhibit Brownian motion in solution as observed by continuous CLSM monitoring (see the video that accompanies this manuscript as part of the SI). While these AF647-capped particles are now stabilized, they still have unbound DNA strands from the complementary partner of $SMDH_4$ on their surfaces that can be used for orthogonal labeling with Cy3, another dye molecule. After the as-prepared AF647-capped particles were mixed with the appropriate Cy3-conjugated DNA strands (5 μM) and incubated at room temperature for 8 h, their CLSM images (Figure 6b, right) clearly show fluorescence signals from both AF647 and Cy3.

Cellular Internalization of Nucleic Acid-Based Polymeric Nanoparticles. Nucleic acid-based polymeric nanoparticles can serve as efficient vehicles for transporting synthetic nucleic acids into cells. Synthetic nucleic acids such as antisense DNA and small interfering RNA have long been used for both gene-regulation study and gene therapy. However, they are not readily uptaken by cells: their high molecular weights and polyanionic backbones sterically and electrostatically impede them from passing through the negatively charged cellular membranes. In addition, they also suffer from a high susceptibility to enzymatic degradation when administered in isolated molecular form. Thus, appropriate delivery systems that can encapsulate the nucleic acids are often used to carry them into cells and protect them from degradation prior to reaching the therapeutic targets inside the cells (e.g., mRNA).

Among the emerging cellular delivery systems, nanoparticles are predicted to have the optimal endocytotic cellular uptake potentials when they are in the 25−30 nm size regimes.[25] Indeed, for synthetic nucleic acid delivery, SNAs in this size

DOI: 10.1021/jacs.5b03485
J. Am. Chem. Soc. 2015, 137, 8184−8191

regime have shown excellent promises in their ability to easily enter into cells through an endocytotic pathway.[2,26−28] Given these precedents, we hypothesize that our nucleic acid-based polymeric nanoparticles in the 25−30 nm size regimes could also be efficiently internalized into cells. In addition, because the synthetic nucleic acids in our nanoparticle are packed throughout the whole volume in a high-density (>98 wt % nucleic acid composition) fashion, capping them, as shown in the previous section, with nuclease-resistant agents may confer good protection of the whole cargo against enzymatic degradation compared to free synthetic nucleic acids.

To evaluate the cellular uptake efficiency of our nucleic acid-based polymeric nanoparticles, we treated SKOV-3 human carcinoma ovarian cells with either a sample that has been capped with an AF647-conjugated ssDNA (total [DNA] = 15 μM; capping [DNA] = 75 nM; D_H = 24 ± 5 nm) or free AF647-conjugated ssDNA (75 nM) for 24 h, and analyzed their cellular uptake by CLSM and flow cytometry. CLSM images (Figure 7a) of the cells that were exposed to the AF647-capped

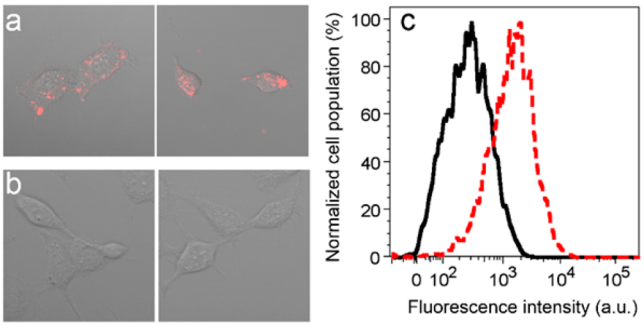

Figure 7. (a,b) CLSM images of SKOV-3 cells after 24 h exposure to either nucleic acid-based polymeric nanoparticles capped with an AF647-conjugated ssDNA (total [DNA] = 15 μM; capping [DNA] = 75 nM; D_H = 24 ± 5 nm) (top image) or free AF647-conjugated ssDNA ([DNA] = 75 nM) (bottom image). The visible red-color regions in the top image indicate high uptake of AF647-capped nucleic acid-based polymeric nanoparticles into cells in contrast to minimal uptake of the free AF647-conjugated ssDNA in the bottom image. (c) Quantitative flow cytometric profiles showing that cellular internalization of the AF647-capped nucleic acid-based polymeric nanoparticles (red) is ten times that of the free AF647-conjugated ssDNA (gray) (2200 vs 230 au, respectively).

nucleic acid-based polymeric nanoparticles clearly shows the localization of AF647-conjugated ssDNA (red-colored regions) inside the cells, indicating successful cellular internalization. In stark contrast, no red region is visually observed in the control sample of cells that were exposed to the free AF647-conjugated ssDNA (Figure 7b). Quantitative analysis by flow cytometry (Figure 7c) further confirmed the CLSM observation by showing that the average AF647-based fluorescence intensity of the cells that were exposed to the nucleic acid-based polymeric nanoparticles is about ten times higher than that of the control (i.e., exposed to free AF647-conjugated ssDNA). Such enhanced cellular uptake may prove to be advantageous in gene delivery applications where increases in the amounts of internalized synthetic nucleic acids can lead to excellent transfection efficiency.

Stability of Nucleic Acid-Based Polymeric Nanoparticles against DNase I. Before evaluating the hypothesis that capping our nanoparticles with nuclease-resistant agents can lead to enhanced protection of the $SMDH_4$ building blocks against attack by nucleases, we first examined the size-dependent resistance of our nucleic acid-based polymeric nanoparticles against DNase I, an endonuclease that is capable of degrading both single- and double-stranded DNA as well as chromatin.[29] Samples of large (D_H = 340 ± 50 nm) and small (D_H = 24 ± 5 nm) nucleic acid-based polymeric nanoparticles, along with a control $SMDH_4$ that has been hybridized with complementary free DNA strands, were exposed to a solution of DNase I (5 units/mL) at 37 °C for 1 h and then denatured and analyzed by polyacrylamide gel electrophoresis (PAGE). As shown in Figure 8a, significant amounts of the $SMDH_4$ remain

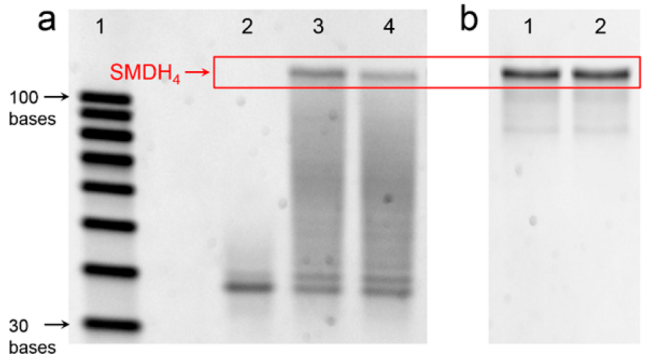

Figure 8. (a) Denaturing PAGE-gel (12%) image of the nucleic acid-based polymeric nanoparticles and a control duplex-hybridized $SMDH_4$ after a 1 h treatment with DNase I (5 units/mL). The control is a discrete $SMDH_4$ that was initially hybridized with a complementary free ssDNA strand prior to DNase I treatment. From left to right: lane 1 = ssDNA ladder; lane 2 = control duplex-hybridized $SMDH_4$; lane 3 = large (D_H = 340 ± 50 nm) nucleic acid-based polymeric nanoparticles, and lane 4 = small (D_H = 24 ± 5 nm) nucleic acid-based polymeric nanoparticles. The samples were run after particle dissolution (i.e., denaturing), showing a significant amount of the $SMDH_4$ building blocks remain intact in the two nanoparticle-derived samples. In contrast, the $SMDH_4$ component of the control has completely degraded. (b) Denaturing PAGE-gel (12%) image of our nucleic acid-based polymeric nanoparticles after particle dissolution, showing that virtually all of the $SMDH_4$ building blocks remain intact during the particle formation process. From left to right: lane 1 = large (D_H = 340 ± 50 nm) nucleic acid-based polymeric nanoparticles and lane 2 = small (D_H = 24 ± 5 nm) nucleic acid-based polymeric nanoparticles.

intact in both nanoparticle samples, suggesting that they are better protected against DNase I than the $SMDH_4$ control, which completely degraded into smaller fragments. As an additional control, the PAGE gel image of denatured samples of both types of nanoparticles showed that virtually all of the $SMDH_4$ building blocks remain intact during the particle formation process (Figure 8b).

That the $SMDH_4$ control qualitatively degraded faster than the small nanoparticles, which in turn degraded faster than the larger ones, can be partially attributed to two size-dependent factors. First, there is a higher probability for the $SMDH_4$ building blocks to encounter the enzyme when existing as individual units (instead of being "packaged" inside the nanoparticles). That is, at the same DNA concentration, the assembly of $SMDH_4$ into nanoparticles ensures that there is a lower number of available DNA-containing entities (either nanoparticles or free $SMDH_4$ units) with which the enzyme can react. Second, the synthetic nucleic acids near the center of the smaller nanoparticle will be exposed to the enzyme faster than those near the center of the larger nanoparticles. We note in

DOI: 10.1021/jacs.5b03485
J. Am. Chem. Soc. 2015, 137, 8184−8191

passing that the high concentration of salts (ion cloud) surrounding the nucleic acid-based polymeric nanoparticles, which repels the binding of the enzyme, can also contribute to the overall enhanced stability of the $SMDH_4$ building blocks inside the nanoparticles. This potential third factor has recently been reported for SNAs,[28,30] and is currently being investigated by us; these results will be reported in due course.

To test the hypothesis that capping our nanoparticles with nuclease-resistant agents, such as poly(ethylene glycol) (PEG), can lead to enhanced protection of the $SMDH_4$ building blocks against attack by nucleases, we employed two types of PEG-conjugated capping ssDNA strands, each with a sequence that is complementary to the two SMDH strands comprising the nucleic acid-based polymeric nanoparticles. Two samples of each particle diameter, i.e., large (D_H = 340 ± 50 nm) and small (D_H = 24 ± 5 nm), were then capped with one or both of these PEG-conjugated capping ssDNA strands using the aforementioned orthogonal functionalization method (SI, Section S3). All four samples were then exposed to the same DNase I treatment described previously in this section (5 units/mL at 37 °C for 1 h), and then denatured and analyzed by polyacrylamide gel electrophoresis (PAGE) to evaluate the effect of relative PEG density. As shown in Figure 9a, most of the dually PEG-capped nanoparticles with large diameters were not degraded and even the dually PEG-capped small nanoparticles were also highly stabilized against the enzyme. Having a higher density of PEG-capping is clearly more advantageous: the singly PEG-capped samples appear to degrade slightly more under the same DNase I treatment regime (Figure 9b). These results again highlight the modular characteristic of our nucleic acid-based polymeric nanoparticles: higher levels of protection of the $SMDH_4$ content can be engineered into their surfaces with higher PEG density. In addition, because PEG chains with two different functional end-groups are readily available, the incorporation of nuclease resistance can be readily incorporated without sacrificing the capacity for orthogonal surface functionalization.

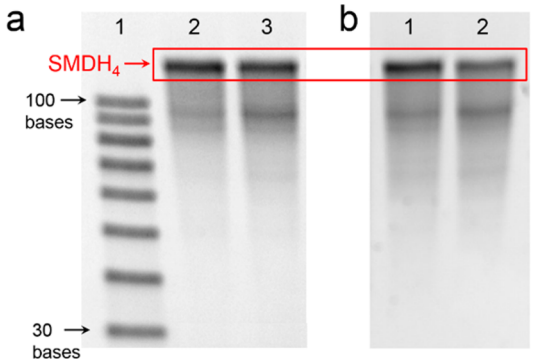

Figure 9. (a) Denaturing PAGE-gel (12%) image of the dually PEG-capped nucleic acid-based polymeric nanoparticles after a 1 h treatment with DNase I (5 units/mL). Lane 1 = ssDNA ladder; lanes 2 and 3 = large (D_H = 340 ± 50 nm) and small (D_H = 24 ± 5 nm) nucleic acid-based polymeric nanoparticles that were dually capped with two PEG-functionalized strands, respectively. Samples were run after particle dissolution (i.e., denaturing). In a qualitative comparison to the gel image shown in Figure 8a, there was much less degradation of the $SMDH_4$ building blocks in these samples into small fragments: most of the $SMDH_4$ in the large nanoparticle samples and a large amount of those in the small sample stay intact. (b) Denaturing PAGE-gel (12%) image of the nucleic acid-based polymeric nanoparticles that have been capped with only one PEG-functionalized strands after a 1 h treatment with DNase I (5 units/mL). Lanes 1 and 2 = large (D_H = 340 ± 50 nm) and small (D_H = 24 ± 5 nm) nucleic acid-based polymeric nanoparticles that were capped with only one PEG-functionalized strand, respectively. Samples were run after particle dissolution. In a qualitative comparison to the gel images shown in Figures 8a and 9a, the $SMDH_4$ building blocks in these samples are slightly less protected than those in the dually PEG-capped samples but much better protected than those in the unprotected samples.

CONCLUSION

In summary, we have shown that tetravalent molecular cores can be used to create tetravalent DNA constructs for rapidly preparing nucleic acid-based polymeric nanoparticles. The size and distributions of these novel nanomaterials can be modulated by tuning the SMDH concentration, the assembly time/temperature, and the NaCl concentration, demonstrating a systematic strategy for constructing nucleic acid nanoparticles from purely organic building blocks without the need for a template or scaffold.[31−34] These nucleic acid-based polymeric nanoparticles exhibit enhanced cellular internalization and can be functionalized to have highly enhanced resistance against DNase I compared to the $SMDH_4$ building blocks. Together with the ability to transform these particles into SNAs, while still maintaining active surface groups for further functionalization, these novel materials have the potential to become useful in areas spanning both diagnostics and therapeutics.

EXPERIMENTAL SECTION

Materials and Instrumentation. See SI, Section S1.

Synthesis of $SMDH_4$s. *(a) Synthesis of Alkyne-Modified ssDNA on CPG Beads.* The alkyne-modified ssDNA on CPG beads were synthesized according to a previously published procedure.[11] Syntheses were carried out from the 3′ direction using controlled pore glass (CPG) beads possessing 1 μmol of either adenine (Glen Research, dA-CPG # 20-2001-10, (1000 Å, 38 μmol/g)) or thymine (Glen Research, dT-CPG # 20-2031-10 (1000 Å, 26 μmol/g)) attached to the surface. The CPG beads were placed in a 1 μmol synthesis column and 3′-phosphoramidites (Glen Research, dA-CE phosphoramidite # 10-1000-C5, Ac-dC-CE phosphoramidite # 10-1015-C5, dmf-dG-CE phosphoramidite # 10-1029-C5, dT-CE phosphoramidite # 10-1030-C5) and 5′-hexynyl phosphoramidite (Glen Research, # 10-1908-90) were then added using the standard 1 μmol protocol on an Expedite 8909 synthesizer to make the CPG-3′-ssDNA-C_4-alkyne (see SI, Table S1 for sequence descriptions). At the end of the synthesis, the beads were dried overnight under a high vacuum, removed from the column, and kept in a tightly capped vial that is filled with dry nitrogen gas. The solid-phase coupling reactions with the tetraazide core were then carried out using these dry CPG beads.

(b) Solid-Phase Synthesis of $SMDH_4$. The as-prepared dry CPG beads containing alkyne-modified DNA (1 μmol) were placed in a 1.5 mL Eppendorf tube. To the tube were sequentially added the tetraazide core (5−7 μmol) in DMF (0.75 mL), tris(3-hydroxypropyltriazolylmethyl)amine (7 μmol) in DMF (0.2 mL), $CuSO_4{\cdot}5H_2O$ (5 μmol) in DMF (0.05 mL), and L-ascorbic acid (10 μmol) in DMF (0.1 mL). The reaction tube was then filled with dry nitrogen gas before being capped and shaken for 18 h at 25 °C in an Thermomixer R (Eppendorf, Hauppauge, NY) instrument at 1200 rpm (Note: the CPG beads should be properly agitated in DMF solution and not allowed to settle at the bottom of the tube during the reaction). The resulting CPG beads were filtered using a one-side-fritted 1 μmol Expedite DNA synthesis column (Glen Research, # 20-0021-01), washed with DMF (10 × 1 mL) and acetone (10 × 1 mL), and dried using a stream of dry nitrogen. The CPG beads containing the products were placed in a vial containing 1 mL of AMA (1:1 v/v

DOI: 10.1021/jacs.5b03485
J. Am. Chem. Soc. 2015, 137, 8184−8191

30% ammonium hydroxide solution:methylamine solution; ***Caution! Only freshly made AMA solutions should be used***), and the vial was capped and heated at 65 °C for 15 min to cleave the SMDHs from the solid supports. The ammonia and methylamine byproducts were then removed by passing a stream of dry nitrogen gas over the content of the vial until the characteristic ammonia smell disappears. The remaining liquid, which contains the crude SMDHs, was collected by pipet and the remaining beads were further extracted with ultrapure deionized water (3 × 200 μL). These extracts were combined with the initial solution of crude SMDHs (affording a total volume of 0.8 mL at the end) and filtered through 0.45 μm nylon syringe filter (Acrodisc 13 mm syringe filter # PN 4426T).

(c) Purification and Characterization of $SMDH_4$s. See SI, Section S2.

Assembly of $SMDH_4$. Equimolar mixtures of the as-prepared $SMDH_4$ and its complementary partner were added into 0.5 mL Eppendorf tubes. Enough Tris·HCl buffer solution (20 mM Tris·HCl with appropriate concentrations of NaCl; pH = 7.4) was then added to make solutions with the desired total concentration of DNA (2, 5, 10, 15, and 100 μM). The resulting solutions were heated to 90 °C in a Thermomixer R 5355 instrument without shaking and kept there for 10 min to remove all initial DNA interactions. The power to the heating block was then turned off to allow the solution to slowly cool to room temperature over 3 h (for a typical cooling profile of this equipment, please see Figure S16 in the SI of the reported publication).[18] The resulting nucleic acid-based polymeric particles were analyzed by DLS and STEM (See SI, Section S3). For other programmable cooling profiles used in the cooling-rate study, a MJ Mini Gradient Thermal Cycler (Bio-Rad Laboratories, Inc., Hercules, CA) was utilized.

Stabilizing Nucleic Acid-Based Polymeric Nanoparticles with Capping DNA Strands. In a typical experiment, an equimolar mixture of the as-prepared $SMDH_4$ and its complementary partner (total [DNA] = 10 or 15 μM) was placed into a 0.5 mL Eppendorf tube. Enough Tris-buffered saline (TBS, 20 mM Tris·HCl and 150 mM NaCl buffer solution, pH 7.4) was then added to make a 0.1 mL solution. This solution was heated to 90 °C in a Thermomixer R 5355 instrument and kept there for 10 min to clear out all initial DNA interactions. The power to the heating block was then turned off to allow the solution to slowly cool to room temperature over 3 h. The cooled-down solution of assembled nucleic acid-based polymeric particles was then mixed with capping DNA strands (5 or 7.5 μM; with or without AF647 dye), and the resulting solution was left at rt for 8 h without shaking. The resulting solution of capped particles was analyzed by DLS and CLSM.

Orthogonal Labeling of Two Dyes onto Nucleic Acid-Based Polymeric Nanoparticles. In a typical experiment, an equimolar mixture of the as-prepared $SMDH_4$ and its complementary partner was placed into a 0.5 mL Eppendorf tube. Enough TBS was then added to make a 0.1 mL solution (total [DNA] = 10 μM). This solution was heated to 90 °C in a Thermomixer R 5355 instrument and kept there for 10 min to clear out all initial DNA interactions. The power to the heating block was then turned off to allow the solution to slowly cool to room temperature over 3 h. The cooled-down solution of assembled nucleic acid-based polymeric particles was then mixed with AF647-conjugated capping DNA strands (final concentration = 5 μM, in stoichiometric equivalence to the total DNA concentration in each of the two $SMDH_4$ assembly partners but in excess of the concentration of unhybridized DNA strands on the surface), and the resulting solution was left at rt for 8 h without shaking to form a solution of AF647-labeled particles. Next, Cy3-conjugated capping DNA strands (final concentration = 5 μM, in stoichiometric equivalence to the total DNA concentration in each of the two $SMDH_4$ assembly partners but in excess of the concentration of unhybridized DNA strands on the surface) were added and the resulting solution was left at rt for 8 h without shaking. The resulting solution of orthogonally labeled particles (with both AF647 and Cy3 fluorophores on the surface) was analyzed by CLSM.

General Cell Culture Conditions. See SI, Section S4.

Cellular Internalization of Nucleic Acid-Based Polymeric Nanoparticles. *(a) Assessment of Cellular Uptake by Flow Cytometry.* SKOV-3 cells (100,000 cells) were plated into each well of 12-well plates and incubated for 24 h. The media were then replaced with preprepared media containing either free AF647-conjugated ssDNA (75 nM, 0.5 mL/well) or nucleic-acid based polymeric nanoparticles (total [DNA] = 15 μM; D_H = 24 ± 5 nm) capped with AF647-conjugated ssDNA (75 nM, 0.5 mL/well). After 24 h incubation, the cells were washed with DPBS (3 × 1 mL/well), treated with a TrypLE Express (1×) solution (0.5 mL/well), harvested, transferred to 1.5 mL microcentrifuge tubes, and centrifuged at 1000 g for 5 min. After removing the supernatant via aspiration, the resulting cell pellets were washed in DPBS (0.5 mL/tube) and resuspended in DPBS media (0.5 mL/tube). The fluorescence intensity of AF647-conjugated ssDNA in collected cells was measured by a flow cytometer (BD LSRII, BD Biosciences, San Jose, CA). Data were analyzed using FlowJo software (Tree Star, Inc., Ashland, OR) to obtain the average fluorescence intensity of collected cells.

(b) Cellular Uptake Assessed by CLSM. SKOV-3 cells (100 000 cells) were plated in 35 mm FluoroDish cell culture dishes (World Precision Instruments, Sarasota, FL) and incubated for 24 h. The media in the dishes were then replaced with preprepared media containing either free AF647-conjugated ssDNA (75 nM, 0.5 mL/well) or nucleic-acid based polymeric nanoparticles capped with AF647-conjugated ssDNA (75 nM, 0.5 mL/well). After 24 h incubation, the cells were washed with DPBS (3 × 2 mL/dish) followed by immediate CLSM imaging.

Stability of Nucleic Acid-Based Polymeric Nanoparticles against DNase I. Two different sizes of nucleic acid-based polymeric nanoparticles (total [DNA] = 15 μM; D_H = 24 ± 5 nm and D_H = 340 ± 50 nm, respectively) as well as a control $SMDH_4$ (total [DNA] = 15 μM) that was hybridized with a complementary free ssDNA strand were prepared using the methods described above. Either the particles (25 μL) or control $SMDH_4$ (25 μL) were then mixed with DNase I (2.5 μL of a 100 units/mL solution). The resulting solutions were diluted to 50 μL and incubated at 37 °C for 1 h. EDTA solution (5 μL of a 0.5 M solution) was then added to quench the DNase I reaction and the resulting mixture was immediately lyophilized. The remaining dried powders were redispersed in a mixture of aqueous urea (5 μL of a 7 M solution) and gel-loading dye solution (5 μL, Life Technologies Division of Thermo Fisher Scientific, Inc., Grand Island, NY), heated at 90 °C for 5 min to denature the assembly, and quickly immersed in an ice bath. The resulting solutions were immediately loaded on denaturing polyacrylamide gel (12 wt %). The gel experiments were carried out in 0.5× TBE buffer at 350 V for 1 h and stained with SYBR Gold (Life Technologies Division of Thermo Fisher Scientific, Inc., Grand Island, NY). Images of the gels were taken using an ImageQuant LAS 4010 Gel Imaging System (GE Healthcare, Pittsburgh, PA).

■ ASSOCIATED CONTENT

Ⓢ Supporting Information

A movie of the fluorescently labeled nucleic acid-based polymeric nanoparticles in solution, descriptions of experimental procedures, MALDI and HPLC data for SMDHs, agarose gel image, DLS graphs, and melting profiles. The Supporting Information is available free of charge on the ACS Publications website at DOI: 10.1021/jacs.5b03485.

■ AUTHOR INFORMATION

Corresponding Author

*stn@northwestern.edu

Present Address

[#]The Dow Chemical Company, 400 Arcola Road, Collegeville, Pennsylvania 19426, United States.

Notes

The authors declare no competing financial interest.

DOI: 10.1021/jacs.5b03485
J. Am. Chem. Soc. 2015, 137, 8184−8191

■ ACKNOWLEDGMENTS

This work is financially supported by the Air Force Office of Scientific Research (under Agreement FA-9550-11-1-65 0275 through the MURI program) and the NIH (NCI CCNE Grant C54CA151880). R.V.T. is a NSF Fellow. This work made use of the EPIC facility (NU*ANCE* Center-Northwestern University), which has received support from the MRSEC program (NSF DMR-1121262) at the Materials Research Center; the International Institute for Nanotechnology (IIN); and the State of Illinois, through the IIN. We thank the reviewers of an original version of this manuscript for helpful suggestions that improved its quality.

■ REFERENCES

(1) Rothemund, P. W. K. *Nature* **2006**, *440*, 297−302.
(2) Cutler, J. I.; Auyeung, E.; Mirkin, C. A. *J. Am. Chem. Soc.* **2012**, *134*, 1376−1391.
(3) Macfarlane, R. J.; O'Brien, M. N.; Petrosko, S. H.; Mirkin, C. A. *Angew. Chem., Int. Ed.* **2013**, *52*, 5688−5698.
(4) Seeman, N. C. *Annu. Rev. Biochem.* **2010**, *79*, 65−87.
(5) Pinheiro, A. V.; Han, D.; Shih, W. M.; Yan, H. *Nat. Nanotechnol.* **2011**, *6*, 763−772.
(6) Yang, Y.; Zhao, Z.; Zhang, F.; Nangreave, J.; Liu, Y.; Yan, H. *Nano Lett.* **2013**, *13*, 1862−1866.
(7) Andersen, E. S.; Dong, M.; Nielsen, M. M.; Jahn, K.; Subramani, R.; Mamdouh, W.; Golas, M. M.; Sander, B.; Stark, H.; Oliveira, C. L.; Pedersen, J. S.; Birkedal, V.; Besenbacher, F.; Gothelf, K. V.; Kjems, J. *Nature* **2009**, *459*, 73−76.
(8) Hamblin, G. D.; Hariri, A. A.; Carneiro, K. M. M.; Lau, K. L.; Cosa, G.; Sleiman, H. F. *ACS Nano* **2013**, *7*, 3022−3028.
(9) Zheng, J.; Birktoft, J. J.; Chen, Y.; Wang, T.; Sha, R.; Constantinou, P. E.; Ginell, S. L.; Mao, C.; Seeman, N. C. *Nature* **2009**, *461*, 74−77.
(10) McLaughlin, C. K.; Hamblin, G. D.; Sleiman, H. F. *Chem. Soc. Rev.* **2011**, *40*, 5647−5656.
(11) Thaner, R. V.; Eryazici, I.; Farha, O. K.; Mirkin, C. A.; Nguyen, S. T. *Chem. Sci.* **2014**, *5*, 1091−1096.
(12) Eryazici, I.; Yildirim, I.; Schatz, G. C.; Nguyen, S. T. *J. Am. Chem. Soc.* **2012**, *134*, 7450−7458.
(13) Aldaye, F. A.; Sleiman, H. F. *J. Am. Chem. Soc.* **2007**, *129*, 13376−13377.
(14) Eryazici, I.; Prytkova, T. R.; Schatz, G. C.; Nguyen, S. T. *J. Am. Chem. Soc.* **2010**, *132*, 17068−17070.
(15) Singh, A.; Tolev, M.; Meng, M.; Klenin, K.; Plietzsch, O.; Schilling, C. I.; Muller, T.; Nieger, M.; Brase, S.; Wenzel, W.; Richert, C. *Angew, Chem., Int. Ed.* **2011**, *50*, 3227−3231.
(16) Meng, M.; Ahlborn, C.; Bauer, M.; Plietzsch, O.; Soomro, S. A.; Singh, A.; Muller, T.; Wenzel, W.; Brase, S.; Richert, C. *ChemBioChem* **2009**, *10*, 1335−1339.
(17) Aldaye, F. A.; Sleiman, H. F. *J. Am. Chem. Soc.* **2007**, *129*, 10070−10071.
(18) Yildirim, I.; Eryazici, I.; Nguyen, S. T.; Schatz, G. C. *J. Phys. Chem. B* **2014**, *118*, 2366−2376.
(19) Shultz, A. M.; Farha, O. K.; Hupp, J. T.; Nguyen, S. T. *Chem. Sci.* **2011**, *2*, 686−689.
(20) Oh, M.; Mirkin, C. A. *Nature* **2005**, *438*, 651−654.
(21) Park, S. Y.; Lytton-Jean, A. K. R.; Lee, B.; Weigand, S.; Schatz, G. C.; Mirkin, C. A. *Nature* **2008**, *451*, 553−556.
(22) Macfarlane, R. J.; Lee, B.; Jones, M. R.; Harris, N.; Schatz, G. C.; Mirkin, C. A. *Science* **2011**, *334*, 204−208.
(23) Seferos, D. S.; Giljohann, D. A.; Hill, H. D.; Prigodich, A. E.; Mirkin, C. A. *J. Am. Chem. Soc.* **2007**, *129*, 15477−15479.
(24) Rosi, N. L.; Giljohann, D. A.; Thaxton, C. S.; Lytton-Jean, A. K. R.; Han, M. S.; Mirkin, C. A. *Science* **2006**, *312*, 1027−1030.
(25) Zhang, S.; Li, J.; Lykotrafitis, G.; Bao, G.; Suresh, S. *Adv. Mater.* **2009**, *21*, 419−424.
(26) Giljohann, D. A.; Seferos, D. S.; Patel, P. C.; Millstone, J. E.; Rosi, N. L.; Mirkin, C. A. *Nano Lett.* **2007**, *7*, 3818−3821.
(27) Giljohann, D. A.; Seferos, D. S.; Prigodich, A. E.; Patel, P. C.; Mirkin, C. A. *J. Am. Chem. Soc.* **2009**, *131*, 2072−2073.
(28) Rosi, N. L.; Giljohann, D. A.; Thaxton, C. S.; Lytton-Jean, A. K.; Han, M. S.; Mirkin, C. A. *Science* **2006**, *312*, 1027−1030.
(29) Weir, A. F. In *Enzymes of Molecular Biology*; Burrell, M. M., Ed.; Methods in Molecular Biology, Vol. 16; Humana Press: New York, 1993; pp 7−16.
(30) Seferos, D. S.; Prigodich, A. E.; Giljohann, D. A.; Patel, P. C.; Mirkin, C. A. *Nano Lett.* **2009**, *9*, 308−311.
(31) Rosi, N. L.; Mirkin, C. A. *Chem. Rev.* **2005**, *105*, 1547−1562.
(32) Roh, Y. H.; Lee, J. B.; Kiatwuthinon, P.; Hartman, M. R.; Cha, J. J.; Um, S. H.; Muller, D. A.; Luo, D. *Small* **2011**, *7*, 74−78.
(33) Cigler, P.; Lytton-Jean, A. K. R.; Anderson, D. G.; Finn, M. G.; Park, S. Y. *Nat. Mater.* **2010**, *9*, 918−922.
(34) Díaz, J. A.; Grewer, D. M.; Gibbs-Davis, J. M. *Small* **2012**, *8*, 873−883.

DOI: 10.1021/jacs.5b03485
J. Am. Chem. Soc. 2015, 137, 8184−8191